Acc. Chem. Res. **2002,** *35,* 332−340

Molecular Dynamics of Acetylcholinesterase

TONGYE SHEN,[†,‡] KAIHSU TAI,[†] RICHARD H. HENCHMAN,[†] AND J. ANDREW MCCAMMON*[,†]

Howard Hughes Medical Institute, Department of Chemistry and Biochemistry, Department of Pharmacology, and Department of Physics, University of California—San Diego, La Jolla, California 92093-0365

Received June 6, 2001

ABSTRACT

Molecular dynamics simulations are leading to a deeper understanding of the activity of the enzyme acetylcholinesterase. Simulations have shown how breathing motions in the enzyme facilitate the displacement of substrate from the surface of the enzyme to the buried active site. The most recent work points to the complex and spatially extensive nature of such motions and suggests possible modes of regulation of the activity of the enzyme.

Introduction

Acetylcholinesterase (AChE) is among the fastest of enzymes. This is an evolutionary consequence of one of its key activities—the hydrolysis of the neurotransmitter acetylcholine (ACh) to terminate signaling in cholinergic synapses, including the neuromuscular junction. The great speed of the enzyme is essential for rapid modulation of synaptic activity.

When the first crystallographic structure of AChE was determined in 1991, it revealed a number of surprising features.[1] Among these was the existence of a long, narrow gorge or channel leading from the surface of the enzyme to the chamber containing the active site. Partway along this passageway, the channel is so narrow in the crystal structure that substrate would have no access to the active site if the enzyme were rigid. This original observation for AChE from the fish *Torpedo californica* has subsequently been reiterated in the AChE from the mouse[2] and human.[3]

That structural fluctuations occur in some proteins to allow ligand binding to otherwise inaccessible sites has long been known. In fact, this was noted to be the case for hemoglobin and myoglobin, among the first proteins whose structures were determined.[4] But how could this be reconciled with the great speed of AChE? A series of molecular dynamics simulations that extend back to 1994 has explored this question. The results of these simulations suggest that the primary channel to the active site opens frequently enough to pose little kinetic penalty for the hydrolysis of the physiological substrate. They also suggest that a variety of secondary channels fluctuate open and shut and allow solvent to move between the primary channel and the surroundings as substrate enters.

More recent molecular dynamics simulations have begun to hint at other dynamical features of the AChE that are relevant to its function. These include a coupling of the primary channel fluctuations to collective fluctuations that involve much of the protein. Such coupling could represent a basis for either static or dynamic allostery in the enzyme. In what follows, we review the results of molecular dynamics simulations of mouse AChE, with special emphasis on the newer results. We conclude with a brief discussion of some outstanding issues.

Cholinesterase Biology

Signaling from nerve to muscle is mediated by ACh in specialized synapses called neuromuscular junctions. The mechanism of this process is as follows (Figure 1). ACh is synthesized from choline and acetyl-CoA and packaged into vesicles in the presynaptic terminal. An action potential arriving at the terminal of the presynaptic neuron triggers the opening of voltage-gated Ca^{2+} channels. Ca^{2+} entering the cytosol stimulates the vesicles to release their ACh by exocytosis into the synaptic cleft. ACh diffuses across the cleft and binds to and activates the postsynaptic receptors, allowing Na^+ and K^+ to diffuse across the membrane and depolarize the cell. AChE quickly degrades ACh to acetate and choline, deactivating the receptor and tapering off the transmitted nerve impulse. Choline is taken up again by the presynaptic terminal for resynthesis of ACh.

The mechanism of AChE largely resembles that of serine proteases. Ser 203 (in mouse AChE) nucleophilically attacks the carbonyl group of ACh, displacing the choline to form an acyl-AChE intermediate. A water molecule then displaces the acyl group to regenerate the enzyme and release acetic acid.

Tongye Shen is a graduate student (C.Phil. of physics/biophysics) at UCSD. He received his B.Sc. (applied physics) from Tsinghua University, China, and M.Sc. (physics) from UCSD. His current research interests include using stochastic methods to study dynamical/static properties of biomolecular systems and statistical physics of complex systems.

Kaihsu Tai was born in Taipei, Taiwan (1977). He received his B.S. (Hon.) from California Institute of Technology (1998) and his M.S. in chemistry from the University of California, San Diego (2000). He is currently a doctoral candidate at UCSD, and a member of the McCammon group. His research projects include simulations of molecular systems in neurobiology.

Richard H. Henchman is currently a postdoc at UCSD. He received his B.Sc. Hons. majoring in theoretical chemistry from the University of Sydney, Australia (1996), and his Ph.D. in physical chemistry from the University of Southampton, UK (2000). His research focuses on developing simulation and analysis methods for biological systems.

J. Andrew McCammon received his B.A. from Pomona College and his Ph.D. in chemical physics from Harvard. He joined the faculty of the University of Houston in 1978, and assumed the M. D. Anderson Chair in 1981. In 1995, he moved to UCSD, where he holds the J. E. Mayer Chair of Theoretical Chemistry. He was appointed an Investigator of the Howard Hughes Medical Institute at UCSD in 2000. His group pursues theoretical and computational studies in molecular biophysics, with a current emphasis on moving toward the understanding of supramolecular and cellular phenomena.

* To whom correspondence should be addressed. E-mail: jmccammon@ucsd.edu.

† Howard Hughes Medical Institute, Department of Chemistry and Biochemistry, and Department of Pharmacology.

‡ Department of Physics.

10.1021/ar010025i CCC: $22.00
Published on Web 01/08/2002

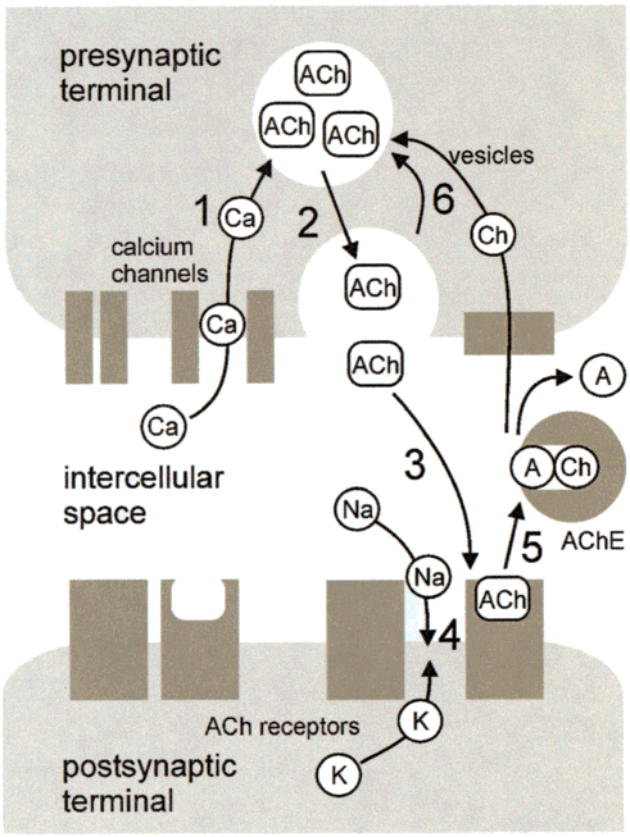

FIGURE 1. Schematic of the neuromuscular synapse. (1) Depolarizing of the cell opens Ca^{2+} channels and Ca^{2+} enters. (2) Ca^{2+}-stimulates vesicles to release acetylcholine (ACh) into the synapse. (3) ACh diffuses and binds to the ACh receptors, opening their ion channels. (4) Na^+ and K^+ diffuse through the channel, depolarizing the postsynaptic terminal. (5) ACh diffuses to acetylcholinesterase (AChE) and is hydrolyzed to choline (Ch) and acetate (A). (6) Ch is taken up for resynthesis of ACh and packaged into vesicles.

AChE is encoded from a single gene but is known to exist in a variety of physiological forms due to alternative mRNA splicing and association with structural subunits.[5,6] Monomer and disulfide-linked dimer forms may be soluble or attached to a membrane by a glycophospholipid. The tetramer form may be soluble, lipid-linked to the membrane, or attached to a collagen triple helix, up to three tetramers per helix.

Clinically, moderate inhibition of AChE is effective in the treatment of a number of diseases to prolong the effect of ACh on the receptor. Such treatment is desirable either if there is reduced concentration of ACh, as in the case of Alzheimer's disease, or if there are fewer receptors, as in the case of myasthenia gravis. Currently, U.S. FDA-approved inhibitors for treatment of Alzheimer's disease are E2020 (donepezil, Aricept), tacrine (Cognex), rivastigmine (Exelon), and galantamine (Reminyl).[7] Inhibitors for treatment of myasthenia gravis include pyridostigmine (Mestinon) and neostigmine (Prostigmine).[8] However, overwhelming inhibition of AChE, particularly by covalent bonding to the active site serine, is invariably lethal. Hence, AChE is a prime target for naturally occurring toxins such as the snake venom fasciculin II, pesticides such as parathion and malathion, and chemical warfare agents such as sarin, tabun, and VX.[9]

Acetylcholinesterase Structure, Dynamics, and Function

The structures of the catalytic domains of the acetylcholinesterases from such species as *T. californica*, mouse, and human are quite similar.[1−3] In all cases, the active site is found at the bottom of a 20 Å long channel leading from the surface of the enzyme, and a group of aromatic side chains forms a bottleneck partway down the channel. Despite these apparent impediments to rapid catalysis, the enzymes hydrolyze acetylcholine at nearly the diffusion-controlled limit. Small, cationic active-site inhibitors can also bind with similarly rapid kinetics. Ligands that are not cationic or that are bulkier can bind in the active site, but with slower kinetics. For example, the effective second-order rate constant k_{cat}/K_m for butyrylthiocholine hydrolysis by mouse AChE is reduced by a factor of 4×10^{-3} relative to the corresponding quantity for the smaller acetylthiocholine of 4.4×10^9 M^{-1} min^{-1}.[10] The second-order rate constant for binding the small, neutral inhibitor TFK by mouse AChE is reduced by a factor of 2×10^{-3} relative to that for a cationic isostere (at zero ionic strength).[11]

One factor that contributes to the speed of binding of cationic ligands to AChE is electrostatics. Early suggestions of an electrostatically enhanced collision rate between such ligands and the enzyme[12] have been confirmed and extended by Brownian dynamics simulations. In the latter, the crystallographic structure of the enzyme serves to define both the target for productive collisions and the enzyme's steric and electrostatic effects on the simulated diffusion of a ligand. Consistent with experiment, such simulations show that steering of a cationic ligand by the field of the enzyme contributes about 2 orders of magnitude to the effective second-order rate constant for binding (cf., e.g., Tara et al.[13]). More recent experimental and simulation studies have shown that the toxin fasciculin II, a small protein that inhibits AChE by binding over the entrance to the gorge, also exhibits electrostatically enhanced, diffusion-controlled binding.[11,14]

But the electrostatic steering effects mentioned above only act to increase the speed of encounter of the cationic ligands with the enzyme. For the ligands to reach the active site, they still must move through the steric bottleneck in the primary channel. And water molecules in the channel must move out of the way of the ligand as it moves along this narrow passageway. To discover mechanisms by which these processes may be facilitated, a series of molecular dynamics simulations of increasing length and quality have been carried out, starting with a 100 ps simulation of the gorge region of the *T. californica* enzyme.[15] This simulation revealed both fluctuations in the width of the bottleneck in the primary channel and the transient opening of a secondary channel—the "back door"—wide enough to allow water molecules to exchange

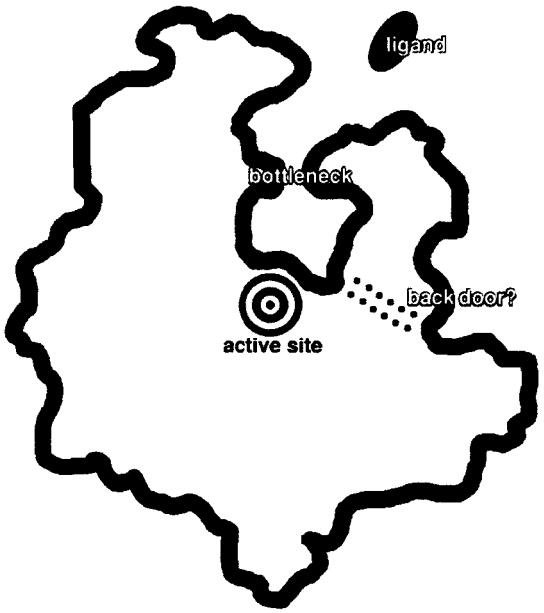

FIGURE 2. Schematic of the AChE monomer. Access of ligands to the active site is governed by fluctuations in the width of the bottleneck in the primary channel or "gorge". Secondary channels ("side" or "back doors") between the active site and the protein surface occur transiently.

between the active site and the exterior of the enzyme (Figure 2). A simulation of the whole *T. californica* dimer for 500 ps was subsequently analyzed in more detail.[16] This simulation confirmed the earlier results and revealed the transient existence of additional possible water exchange pathways between the active site region and the exterior through comparatively thin sections of the gorge.

Statistics gathered from the 500 ps simulation suggested that the distribution of the widths of the bottleneck region in the main channel was essentially Gaussian, with the bottleneck open wide enough to admit acetylcholine less than 5% of the time. Thus, the binding of substrate is a "gated" process. Early theories of such processes indicate that the gating may greatly reduce the rate of ligand binding if the time for diffusional escape of the ligand from the gate region is short compared to the time for the gate to open and close, but the kinetic penalty for gating may be small in the opposite case.[17,18] An analysis was made of AChE kinetics using the data from the 500 ps simulation, plus a simple model of the gate dynamics as diffusion in a harmonic potential.[19] The results indicated that the catalytic rate for the physiologic substrate acetylcholine would, in fact, only be reduced by a factor of about 0.5 due to the gating but that larger substrates would be strongly selected against—a phenomenon characterized as "dynamic selectivity".[20]

As will be seen in what follows, even longer simulations of AChE have started to reveal the dynamical complexity expected for molecules that have rough energy landscapes. Many of the features described above may be preserved, but this requires more detailed study.

The Bottleneck Fluctuations Are Complex

For the last 30 years or so, researchers from different fields have investigated complex systems characterized by rough energy landscapes. Such systems include protein molecules.[21] Full understanding of the activity of a protein therefore requires identification of its functionally important conformational substates and the dynamics of the transitions from one substate to another.

Computer simulation is an important complement to theoretical and experimental study of complex systems, but very long simulations are often required. In the 1980s, a simulation of spin glasses[22] first showed the kinds of complex features inherent in these systems, such as the stretched exponential relaxation behavior above the glass transition temperature, T_g, and even slower power-law decay below T_g. However, simulations of structural glasses were much more difficult.[23] It was not possible until recently to run simulations long enough to explore the rough energy landscape, nor could a large enough system be modeled to eliminate strong boundary effects and produce complex behavior. With increasing computer power in the 1990s, complexity arising from the energy landscape began to be observed in both structural glass and protein simulations.[23,24] Our most recent simulation of AChE, continued for 10 ns, shows clear evidence of the kind of complexity described above. This simulation comprised the monomeric AChE from mouse (543 residues) and more than 25 000 water molecules.[25] State-of-the-art methods, including particle-mesh Ewald treatment of the electrostatic interactions, were used for the simulation.

A key goal of this new simulation was a more accurate description of the dynamics of the bottleneck region of the main channel or gorge. We quantified the gorge width with the single variable, the gorge radius, $\rho(t)$, for snapshots recorded every picosecond from the molecular dynamics trajectory. The gorge radius for each snapshot is defined to be the radius of the largest spherical ligand that can pass through the bottleneck of the gorge and reach the active site chamber. This quantity may be found by generating a solvent-accessible surface using a probe radius of ligand size. An open state is one in which the surface in the active site connects with the bulk, while in the closed state, the surface is cut off from the bulk. Figure 3a and b shows representative open and closed conformations, respectively, for a ligand of a given size. The radius of the probe is then varied to the desired precision to determine the critical radius at which the gorge goes from open to closed, and this is defined to be $\rho(t)$. The variation of $\rho(t)$ with time is plotted in Figure 4. This figure excludes the initial equilibration time in the simulation. The average gorge radius $\langle r(t)\rangle_t = 1.5$ Å. $\rho(t)$ is bounded by $\rho_{max} = 2.4$ Å and $\rho_{min} = 0.8$ Å. The standard deviation is 0.26 Å.

The dynamics of the fluctuating bottleneck were analyzed in three ways. The autocorrelation function of $\rho(t)$ is shown in Figure 4 and reveals a nonexponential relaxation from the normalized initial value of 1.0 since it

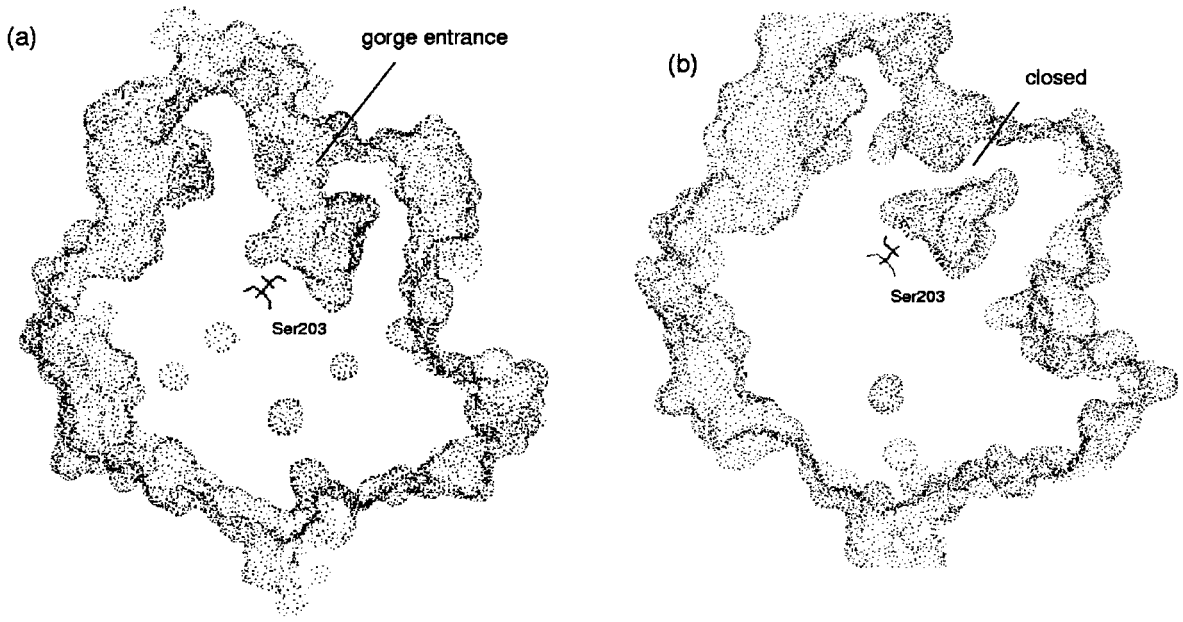

FIGURE 3. Comparison of conformations with an open (a) and closed (b) gorge using a dotted molecular surface representation of AChE. Ser 203 in the active site is shown in the center of each figure.

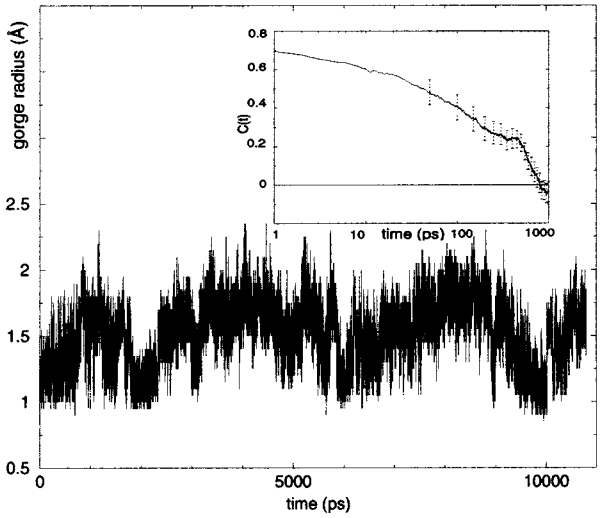

FIGURE 4. Variation of gorge radius during the 10 ns simulation time. The inset shows the time autocorrelation function of the gorge radius. The error bar is a rough estimation based on the assumption that each of the 500 ps blocks of data is independent. Adapted from ref 28 with permission.

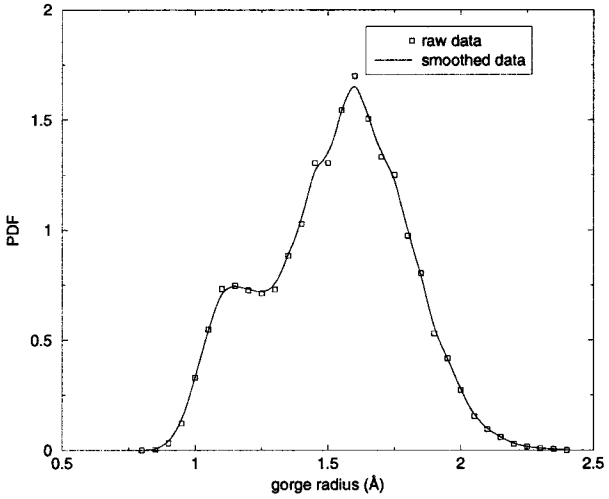

FIGURE 5. Probability density function of the gorge radius. The function has a bimodal shape which indicates that the protein has two major conformational substates with different gorge radii. Reprinted with permission from ref 28. Copyright 2001 American Institute of Physics.

features a fast initial decay followed by a very slow decay. The power spectrum[26] of $\rho(t)$ and the dynamic scaling exponent for a fractional random walk[27] also both show that the gorge fluctuations have the features of fractional Brownian motion. For ideal fractional Brownian motion, all three methods should give power-law functions with exponents which are not independent but instead satify a set of mutual equations.[27] In practice, it seems that dynamic scaling exponents are best among them to overcome the finite-size effect.[27,28]

Further, the form of the probability density function, $P(\rho)$, is instructive. This quantity indicates the relative probability of finding a gorge radius with a given value, ρ. Plotted in Figure 5, $P(\rho)$ shows an interesting bimodal distribution which suggests that there are two major conformational states, one around $\rho = 1.6$ Å and a second around 1.15 Å. The manifestation of complexity is even more evident by examining the transition rate between these two states. Defining a threshold to separate the two conformation states at gorge radius $\rho^* = 1.27$ Å (the position of local minimum between the peaks), the first passage time distributions from one state to the other were calculated. The probability of a transition does not follow an exponential decay, as would be expected for a simple barrier-crossing event, but rather is better described by a power law with small oscillations over several orders of time scale.[28] This kind of complex fluctuation behavior might be a very important aspect of protein motion in

general. A similar kind of molecular-level gating motion might be a candidate for the fractal gating phenomena in the ion channel case which was also proposed from recent experimental results.[29]

Though a challenging problem, there are several recent theories that attempt to explain the nonexponential dynamical nature of complex systems, with varying levels of success.[30−32] Indeed, it is debatable whether there is a universal mechanism leading to power-law or stretched exponential decay in different complex systems. For the case of proteins,[31] it is possible that the power-law behavior may be explained by the hierarchical structure of protein energy landscapes which result from different scales of interactions that all have important but competing contributions. The dynamical constraint hierarchical model[30,32] is one such model that describes the complex relaxation event as a hierarchy of simple Markov relaxations. The hierarchy of relaxations is divided into tiers. In each tier, the relaxations are considered to be parallel and uncorrelated. One tier comprises the fastest degrees of freedom that involve simpler motions of only a few atoms, while another tier consists of the slower motions of a larger group of atoms such as a subdomain. The key feature is that relaxations in the slower tiers are permissible only when the faster tiers have moved into the required conformations. Combining all these effects together, the overall result may appear as a nonexponential decay process typical of a complex system.

The Bottleneck Fluctuations Reflect Collective Motion

Our 10 ns mouse AChE molecular dynamics simulation is also able to provide information about the extent of the of protein motions responsible for the fluctuations in the width of the gorge. The distance between atoms Phe 338 $C_{\epsilon 2}$ and Tyr 124 O_H, both at the constriction point in the bottleneck region, was found to correlate very significantly with the gorge radius, $\rho(t)$, with a correlation coefficient of 0.91. The correlation coefficient for the distance between atoms Phe 338 C_α and Tyr 124 C_α ($d_{124,338}$) and $\rho(t)$ is 0.55. Therefore, the local motions of the side chains projecting into the gorge seem to contribute significantly to the opening of the gorge. But these side chains are riding on larger domains of collective dynamics whose motion is reflected in the C_α displacements, as discussed below. Principal component analysis[33,34] (PCA) provides one way of extracting large-scale motions in proteins. Similar in spirit to a normal-mode analysis, PCA breaks up the total motion into contributions, each with a pattern of coherent motion. Typically, only the motions of the C_α's are included, since the aim is to extract only large-scale motion. We wanted to establish a connection between the principal components and the gorge radius and determine whether only a few components were significant to the gorge breathing motion. Therefore, since $d_{124,338}$ was found to correlate with the gorge radius, we derived an expression for this distance as an exact function of the principal components in the form

$$[d_{124,338}(t)]^2 = S + \sum_{c=1}^{3N} R_c p_c(t) + \sum_{c_1=1}^{3N}\sum_{c_2=1}^{3N} Q_{c_1c_2} p_{c_1}(t) p_{c_2}(t)$$

N is the number of α carbons in the protein; $p_{c_i}(t)$ is the projection or value of principal component c_i at time t; the coefficients S, R_c, and $Q_{c_1c_2}$ are functions of the average positions, $\langle \mathbf{x}_i \rangle_t$, and the matrix of principal component eigenvectors, and thus are time independent.

The first issue to resolve was the relative importance of the three terms that make up $[d_{124,338}(t)]^2$. The constant term, S, corresponds to the average width of the gorge and is not relevant for studying fluctuations. By calculating and comparing the sizes of the linear term, $\sum_c R_c p_c(t)$, and the cross term, $\sum_{c_1}\sum_{c_2} Q_{c_1c_2} p_{c_1}(t) p_{c_2}(t)$, as a function of time, it was observed that both terms make large contributions to the fluctuations in $[d_{124,338}(t)]^2$, often with comparable magnitude but opposite sign. Therefore, a naive model that ignores the contribution of either the cross term or the linear term to the gorge opening behavior is not justified.

The size of the coefficients themselves indicates which principal components contribute the most to fluctuations in $[d_{124,338}(t)]^2$. It was hoped that only a few coefficients would be significant. However, when sorted, neither the R_c or $Q_{c_1c_2}$ coefficients displayed a dominant term or collection of terms. Thus, no few principal components appear to control the fluctuations in the width of the gorge. Nevertheless, such a result is in accord with the complex hierarchical dynamics suggested in the previous section. Therefore, a different approach was needed to make sense out of the complex motions contributing to the gorge radius fluctuations.

We devised an alternative measure to identify and visualize the residues important to gorge fluctuations by calculating a correlation vector for each residue and displaying these on the protein to produce a "porcupine" plot.[25] This was done by defining the correlation coefficient, r_{xi}, between the x coordinate of the C_α of residue i and the gorge radius $\rho(t)$ to be

$$r_{xi} = \frac{\langle (x_i(t) - \langle x_i \rangle_t)(\rho(t) - \langle \rho \rangle_t) \rangle_t}{\sqrt{\langle (x_i(t) - \langle x_i \rangle_t)^2 \rangle_t \langle (\rho(t) - \langle \rho \rangle_t)^2 \rangle_t}}$$

Similar expressions are obtained for r_{yi} and r_{zi} for the y and z coordinates. Note that a negative correlation coefficient does not imply a negative correlation in the traditional sense, but rather that the residue is displaced in the negative coordinate direction from its average position when the gorge is more open than average. These three correlation coefficients make up a correlation vector for the C_α atom of each residue. The size of the correlation vector indicates the extent to which the displacement of the residue and the gorge radius are correlated. The direction of the vector indicates where the residue is displaced when the gorge radius is above average.

The correlation vector for each residue was then displayed on the initial structure with the origin of each vector at the C_α, as shown in Figure 6. This figure reveals

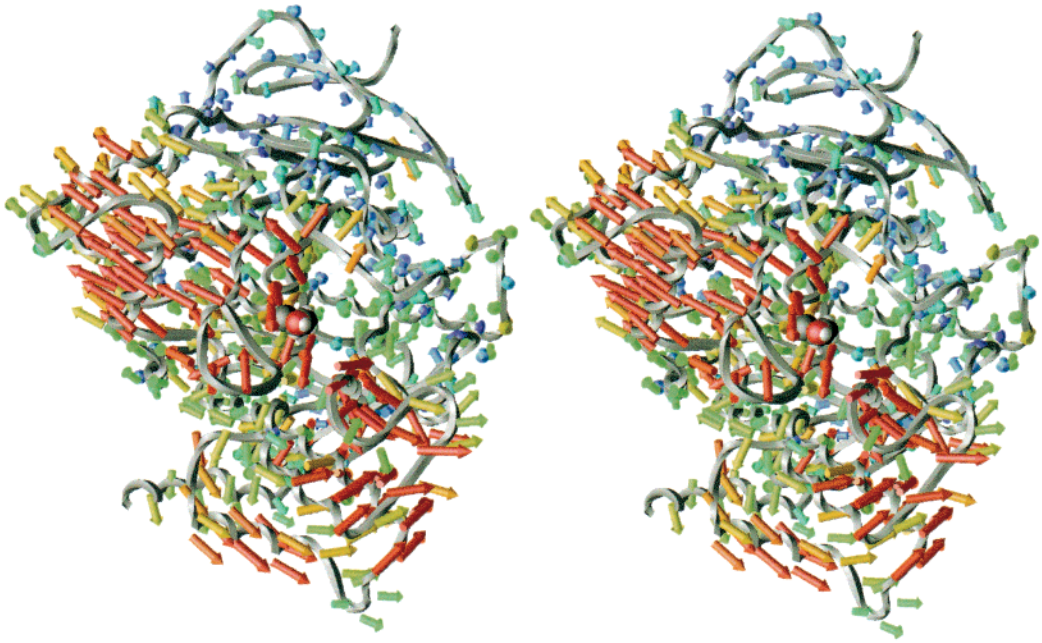

FIGURE 6. Stereograph showing the correlation vector (see text for definition) for each residue of AChE. The vectors are colored by their length, with the longest being red and the shortest blue. The N-terminus is on the top right, and the C-terminus is on the bottom left. The viewer is looking into the gorge, with the active site Ser 203 marked by the space-filling model. Reprinted with permission from ref 40. Copyright 2001 Springer-Verlag.

a wealth of information about protein motions correlated with the gorge. The most surprising feature is that at least half the protein appears to be involved in opening the gorge, as shown by all the high correlation red arrows, some of them quite distant from the gorge. Clearly, it is not simply a matter of a few side chains moving that opens up the gorge, but rather the concerted motion of a large number of residues away from their average positions. Another noteworthy feature is that the direction of residue displacement is approximately radial and away from the gorge, marked by the active site Ser 203. This is a fairly intuitive result, but it does demonstrate that the method is able to extract meaningful information. A similar figure (not shown) was made for entire secondary structure elements, each of whose correlation vector is an average of all their component C_α's. The similar results obtained from this clarified the fact that the motions are largely occurring at the interface between secondary and tertiary structure. Therefore, the porcupine plots provide a solid means to resolve the complex motions of mAChE and to identify potential target residues to modulate the gorge fluctuations.

Water Behavior and Its Access to the Gorge

In addition to the difficulties of navigating the narrow gorge, a ligand must somehow displace water molecules resident in the gorge in order to enter. In more solvent-exposed active sites or other enzymes, highly mobile water molecules are unlikely to interfere with the diffusion of comparably larger ligands. However, in the highly confined gorge of AChE, water molecules may present a significant obstacle to ligand entry. The 10 ns simulation of explicitly solvated AChE provides an opportunity to examine the unusual properties of the gorge water. The simulation is able to provide information about the gorge population, the extent and frequency of the population fluctuations, the means by which waters enter and leave the gorge, and the gorge water structure and dynamics. This information may be related not only to how ligands enter and leave the gorge, but also to how water structure may influence the overall stability of ligands binding in the gorge.[35]

Gorge waters are defined as those waters in the active site chamber separated from the bulk by the bottleneck. More precisely, gorge waters are defined to be within 4 Å of each other and having the minimal number of 4 Å contacts with bulk water. To reduce noise arising from the fuzzy boundary at the bottleneck, a water left or entered the gorge only if the change was maintained for 10 ps. The most common gorge population defined in this way is 20 waters, and the variation in population extends from 16 to 22 waters. A total of 69 population changes occurred during the entire 10 ns. Given the large number of transitions, it should be pointed out that, while many molecular processes are currently beyond the time scale of molecular dynamics, water transitions around proteins is one property for which reasonable statistics are now attainable.

The changes in gorge water population arise from two sources. Waters may enter and exit from the bulk or from the protein. Gorge/bulk transits were observed 53 times, so an estimate of the time scale of this process is ~200 ps. All the transits occurred through the main gorge entrance, the only entrance observed in the crystal

structure. However, previous simulations have revealed other entrances to the gorge that open wide enough for water passage but without any water transits into the gorge.[15,16,36,37] The most frequently observed alternative path in simulations including this one has been the back door at the bottom of the gorge. A second neighboring back door was also observed here and in a simulation of *T. californica* AChE dimer complexed with tacrine.[16] Another front door adjacent to the main gorge entrance was also detected, previously unreported in the literature. However, consistent with previous simulations without a ligand, no side doors were found. Such doors have been seen only when AChE is complexed with the ligands huperzine A[36] and tacrine.[16] Free energy calculations[38] have also suggested that a third front door is favorable for passage of negatively charged acetate. For all simulations, no passages apart from the main gorge were open for more than a small fraction of the simulation time. However, this does not rule out their role in water or product release, since all the simulation times are very short compared to the turnover time of ~0.5 ms for mouse AChE.[11]

The alternative means of water entering the gorge is gorge/protein transits. Four of these involved the real displacement of a water molecule. One site participating in these transits lies behind the catalytic Ser 203 and the other behind Trp 86, a key residue that contributes substantially to the gorge (see Figure 7 discussed further on). Both sites filled and emptied once each during the simulation, indicating that the time scale for waters exchanging with these sites is ~5 ns. Twelve gorge/protein transits were more artifactual and arose when the movement of a neighboring gorge water stranded neighboring water molecules in the protein. Thus, they reflect subtle changes in gorge water packing rather than a change in gorge population.

We have undertaken a more detailed analysis of the gorge water structure and dynamics to get insight into how a ligand may behave in the gorge. This was done by first defining discrete water sites in the gorge. The sites were derived using a recently developed method that places them at peaks in the water density calculated in coordinates local to the gorge.[39] The gorge contains 20 such sites, consistent with a predominant population of 20. Entry of a ligand into the gorge requires empty space and/or moving waters. We have therefore examined the water molecule occupancies, residence times, and traffic between the water sites. The average occupancy of each site was 1.01. However, sites were not always found to be singly occupied. Four of the sites were empty for more than 20% of the simulation time. Two of these sites were at the gorge entrance, while two lay in the middle of the gorge near Glu 202. On the other hand, five sites were doubly occupied 15% of the time. These were fairly evenly distributed over the gorge, again with a tendency to lie in the middle. The next site property studied was average site residence times, illustrated in Figure 7. Residence times in the gorge varied over a wide range from 50 ps (red sites) to the full simulation time of 10 ns (blue sites).

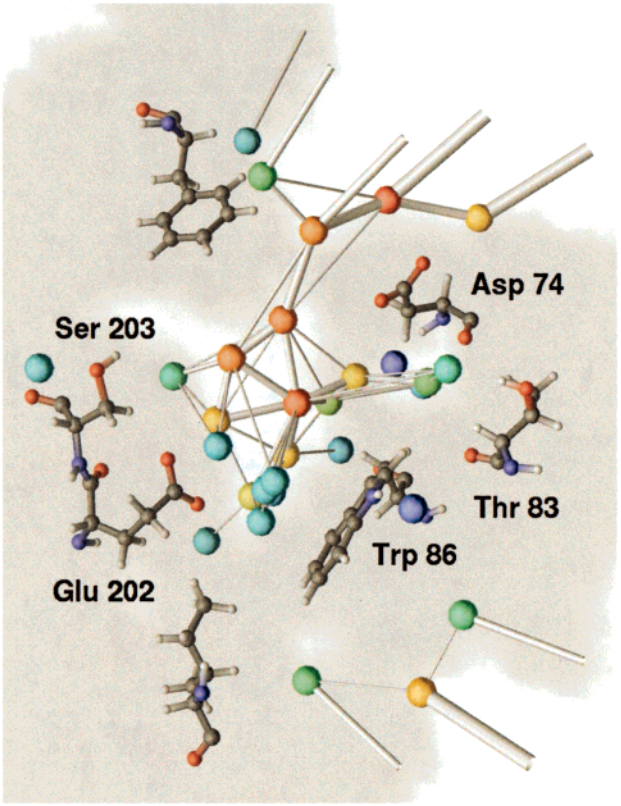

FIGURE 7. Location of the water sites (spheres) and water traffic between them (bars) in and adjacent to the gorge. The color of the site indicates the average residence time of the site (red ~50 ps to blue ~10 ns). The thickness of the bar indicates the number of waters that pass along the bar (thinnest < 10 to thickest ~50; bars with less than three transits are excluded for clarity). The gray background represents a cross section of the protein.

The mobile areas are the gorge center, entrance, and face of Trp 86, while the pocket between Thr 83 and Asp 74 and the choline binding site are the least mobile, the latter possibly due to the presence of the sodium ion. Finally, the water traffic between sites may also be analyzed. This is also shown in Figure 7 by the bars connecting sites. The thickness scales with the number of water transits. Again, most of the traffic involves waters exchanging with the center of the gorge or through the main gorge entrance. Few waters diffuse directly along the protein surface.

The main result is that the center and entrance of the gorge are characterized by shorter residence times, more traffic, and a higher chance of empty or double occupancy, and they contribute the most to fluctuations in gorge water population. Such properties are expected to be key to ligand entry. The sides of the gorge mostly have the opposite properties, the exceptions being sites beside Glu 202 and the face of Trp 86, which may contain waters of lower stability suitable for displacement by ligands.

To understand how water mobility would affect ligands entering the gorge, the diffusion coefficient was roughly estimated along an axis leading from the gorge to the bulk, assuming one-dimensional diffusion. The diffusion coefficient plunges dramatically inside the gorge compared to bulk by up to a factor of 100. Assuming that the

diffusion coefficient of acetylcholine behaves similarly, its diffusion coefficient in the gorge would be $\sim$0.6 Å^2 ns^{-1}, 100 times smaller than its value in bulk water of $\sim$60 Å^2 ns^{-1}. Using the Einstein diffusion relation in one dimension, acetylcholine should diffuse into the gorge, a length of about 15 Å, in $\sim$200 ns. This is still negligible compared to the turnover time of the enzyme, $\sim$0.5 ms.[11] Therefore, given the nanosecond time scale of water and the $\sim$100 ns time scale of the ligand diffusing into the gorge, these relatively rapid steps are not inconsistent with the great speed of AChE.

Concluding Remarks

The results described above suggest that the dynamics of the bottleneck in the primary channel or gorge of AChE influence the binding of ligands to the active site. For the normal state of the enzyme, the bottleneck fluctuations are likely not to hinder the binding of ACh significantly, but larger ligands may escape by diffusion before a large enough fluctuation allows binding. We call this "dynamic selectivity". Additional simulation studies, with substrate models included, are needed to explore these possibilities further.

The bottleneck dynamics in part reflect complex, collective motion of a large fraction of the protein. This raises the possibility that alterations at the AChE surface, e.g., by the binding of protein toxins, could alter the kinetics of substrate transport through the bottleneck to produce allosteric effects.

The dynamic selectivity that has been suggested for binding of ligands to the active site could represent a more general phenomenon in biomolecular recognition. For example, protein−protein association that involves internal structural rearrangements in the monomers could display kinetic signatures of the competition between the internal and overall structural changes.

We are grateful to Dr. Tjerk Straatsma for his continuing help with the molecular dynamics components of the NWChem software. K.T. holds a fellowship from the La Jolla Interfaces in Science Program, which is supported in part by the Burroughs-Wellcome Fund. This work has also been supported in part by grants from NSF, the San Diego Supercomputer Center, NBCR, HHMI, and the W. M. Keck Foundation.

References

(1) Sussman, J. L.; Harel, M.; Frolow, F.; Oefner, C.; Goldman, A.; Toker, L.; Silman. Atomic structure of acetylcholinesterase from *Torpedo californica*: A prototypic acetylcholine-binding protein. *Science* **1991**, *253*, 872−879.

(2) Bourne, Y.; Taylor, P.; Marchot, P. Acetylcholinesterase inhibition by fasciculin: Crystal structure of the complex. *Cell* **1995**, *83*, 503−512.

(3) Kryger, G.; Harel, M.; Giles, K.; Toker, L.; Velan, B.; Lazar, A.; Kronman, C.; Barak, D.; Ariel, N.; Shafferman, A.; Silman, I.; Sussman, J. L. Structures of recombinant native and E202Q mutant human acetylcholinesterase complexed with the snake-venom toxin fasciculin-II. *Acta Crystallogr.* **2000**, *D56*, 1385−1394.

(4) Perutz, M. F.; Mathews, F. S. An x-ray study of azide methaemoglobin. *J. Mol. Biol.* **1966**, *21*, 199−202.

(5) Massoulié, J.; Pezzementi, L.; Bon, S.; Krejci, E.; Vallette, F. Molecular and cellular biology of cholinesterases. *Prog. Neurobiol.* **1993**, *41*, 31−91.

(6) Taylor, P.; Radić, Z. The cholinesterases: from genes to proteins. *Annu. Rev. Pharmacol. Toxicol.* **1994**, *34*, 281−320.

(7) Grutzendler, J.; Morris, J. C. Cholinesterase inhibitors for Alzheimer's disease. *Drugs* **2001**, *61*, 41−52.

(8) Wittbrodt, E. T. Drugs and myasthenia gravis: an update. *Arch. Intern. Med.* **1997**, *157*, 399−408.

(9) Taylor, P. In *The Pharmacological Basis of Therapeutics*; Hardman, J. G., Limbird, L. E., Molinoff, P. B., Ruddon, R. W., Gilman, A. G., Eds.; McGraw-Hill: New York, 1996; pp 161−176.

(10) Vellom, D. C.; Radić, Z.; Li, Y.; Pickering, N. A.; Camp, S.; Taylor, P. Amino acid residues controlling acetylcholinesterase and butyrylcholinesterase specificity. *Biochemistry* **1993**, *32*, 12−17.

(11) Radić, Z.; Kirchhoff, P. D.; Quinn, D. M.; McCammon, J. A.; Taylor, P. Electrostatic influence on the kinetics of ligand binding to acetylcholinesterase: Distinctions between active center ligands and fasciculin. *J. Biol. Chem.* **1997**, *272*, 23265−23277.

(12) Nolte, H. J.; Rosenberry, T. L.; Neumann, E. Effective charge on acetylcholinesterase active sites determined from the ionic strength dependence of association rate constants with cationic ligands. *Biochemistry* **1980**, *19*, 3705−3711.

(13) Tara, S.; Elcock, A. H.; Kirchhoff, P. D.; Briggs, J. M.; Radić, Z.; Taylor, P.; McCammon, J. A. Rapid binding of a cationic active site inhibitor to wild type and mutant mouse acetylcholinesterase: Brownian dynamics simulation including diffusion in the active site gorge. *Biopolymers* **1998**, *46*, 465−474.

(14) Elcock, A. H.; Gabdoulline, R. R.; Wade, R. C.; McCammon, J. A. Computer simulation of protein−protein association kinetics: Acetylcholinesterase-fasciculin. *J. Mol. Biol.* **1999**, *291*, 149−162.

(15) Gilson, M. K.; Straatsma, T. P.; McCammon, J. A.; Ripoll, D. R.; Faerman, C. H.; Axelsen, P. H.; Silman, I.; Sussman, J. L. Open "back door" in a molecular dynamics simulation of acetylcholinesterase. *Science* **1994**, *263*, 1276−1278.

(16) Wlodek, S. T.; Clark, T. W.; Scott, L. R.; McCammon, J. A. Molecular dynamics of acetylcholinesterase dimer complexed with tacrine. *J. Am. Chem. Soc.* **1997**, *119*, 9513−9522.

(17) McCammon, J. A.; Northrup, S. H. Gated binding of ligands to proteins. *Nature* **1981**, *293*, 316−317.

(18) Szabo, A.; Shoup, D.; Northrup, S. H.; McCammon, J. A. Stochastically gated diffusion-influenced reactions. *J. Chem. Phys.* **1982**, *77*, 4484−4493.

(19) Zhou, H.; Wlodek, S.; McCammon, J. Conformation gating as a mechanism for enzyme specificity. *Proc. Natl. Acad. Sci. U.S.A.* **1998**, *95*, 9280−9283.

(20) McCammon, J. A. Are molecular motions important for function? In *Simplicity and Complexity in Proteins and Nucleic Acids*; Frauenfelder, H., Deisenhofer, J., Wolynes, P. G., Eds.; Dahlem University Press: Berlin, 1999; pp 193−198.

(21) Frauenfelder, H., Deisenhofer, J., Wolynes, P. G., Eds. *Simplicity and Complexity in Proteins and Nucleic Acids*; Dahlem University Press: Berlin, 1999.

(22) Ogielski, A. T. Dynamics of three-dimensional Ising spin glasses in thermal equilibrium. *Phys. Rev. B: Condens. Matter Mater. Phys.* **1985**, *B32*, 7384−7398.

(23) Phillips, J. C. Stretched exponential relaxation in molecular and electronic glasses. *Rep. Prog. Phys.* **1996**, *59*, 1133−1207.

(24) Kuczera, K.; Lambry, J.; Karplus, M. Nonexponential relaxation after ligand dissociation from myoglobin: A molecular dynamics simulation. *Proc. Natl. Acad. Sci. U.S.A.* **1993**, *90*, 5805−5807.

(25) Tai, K.; Shen, T.; Börjesson, U.; Philippopoulos, M.; McCammon, J. A. Analysis of a 10-nanosecond molecular dynamics simulation of mouse acetylcholinesterase. *Biophys. J.* **2001**, *81*, 715−724.

(26) Weissman, M. 1/f noise and other slow, nonexponential kinetics in condensed matter. *Rev. Mod. Phys.* **1988**, *60*, 537−571.

(27) Peng, C.-K.; Buldyrev, S. V.; Goldberger, A. L.; Havlin, S.; Simons, M.; Stanley, H. E. Finite-size effects on long-range correlations: Implications for analyzing DNA sequences. *Phys. Rev. E: Stat. Phys., Plasmas, Fluids, Relat. Interdiscip. Top.* **1993**, *E47*, 3730−3733.

(28) Shen, T. Y.; Tai, K.; McCammon, J. A. Statistical analysis of the fractal gating motions of the enzyme acetylcholinesterase. *Phys. Rev. E: Stat. Phys., Plasmas, Fluids, Relat. Interdiscip. Top.* **2001**, *E63*, 041902(6).

(29) Bezrukov, S. M.; Winterhalter, M. Examining noise sources at the single-molecule level: 1/f noise of an open maltoporin channel. *Phys. Rev. Lett.* **2000**, *85*, 202−205.

(30) Palmer, R. G.; Stein, D. L.; Abrahams, E.; Anderson, P. W. Models of hierarchically constrained dynamics for glassy relaxation. *Phys. Rev. Lett.* **1984**, *53*, 958−961.

(31) For a brief review of protein systems, see: Dewey, T. G. *Fractals in Molecular Biophysics*; Oxford University Press: New York, 1997; Chapters 6 and 7.

(32) Nonnenmacher, T. F.; Nonnenmacher, D. J. F. A fractal scaling law for protein gating kinetics. *Phys. Lett. A* **1989**, *140*, 323−326.
(33) García, A. E. Large-amplitude nonlinear motions in proteins. *Phys. Rev. Lett.* **1992**, *68*, 2696−2699.
(34) Amadei, A.; Linssen, A. B.; Berendsen, H. J. Essential dynamics of proteins. *Proteins* **1993**, *17*, 412−425.
(35) Koellner, G.; Kryger, G.; Millard, C. B.; Silman, I.; Sussman, J. L.; Steiner, T. Active-site gorge and buried water molecules in crystal structures of acetylcholinesterase from *Torpedo californica*. *J. Mol. Biol.* **2000**, *296*, 713−735.
(36) Tara, S.; Helms, V.; Straatsma, T. P.; McCammon, J. A. Molecular dynamics of mouse acetylcholinesterase complexed with huperzine A. *Biopolymers* **1999**, *50*, 347−359.
(37) Tara, S.; Straatsma, T. P.; McCammon, J. A. Mouse acetylcholinesterase unliganded and in complex with huperzine A: A comparison of molecular dynamics simulations. *Biopolymers* **1999**, *50*, 35−43.
(38) Enyedy, I. J.; Kovach, I. M.; Brooks, B. R. Alternate pathways for acetic acid and acetate ion release from acetylcholinesterase: a molecular dynamics study. *J. Am. Chem. Soc.* **1998**, *120*, 8043−8050.
(39) Henchman, R. H.; McCammon, J. A. Extracting hydration sites around proteins from explicit water simulations. *J. Comput. Chem.*, in press.
(40) Baker, N.; Tai, K.; Henchman, R.; Sept, D.; Elcock, A.; Holst, M.; McCammon, J. A: Mathematics and molecular neurobiology. In *Computational Methods for Macromolecules: Challenges and Applications*; Proceedings of the 3rd International Workshop on Algorithms for Macromolecular Modeling, New York City, October 12−14, 2000; Springer-Verlag: Berlin, 2002, in press.

AR010025I